

## Numerical Simulation of Flow Around An Elliptical Cylinder at High Reynolds Numbers

Manish Rawat<sup>1</sup>, Dr. Rajesh Gupta<sup>2</sup> and Dr. R.M.Sarviya<sup>3</sup>

<sup>1</sup> PG Student, <sup>2</sup> Associate Professor, <sup>3</sup> Professor  
<sup>1-3</sup> Department of Mechanical Engineering,  
Maulana Azad National Institute of Technology, Bhopal,  
MP-462051, India

### Abstract

High Reynolds number flows ( $Re = 0.5 \times 10^6$ ,  $1 \times 10^6$ ,  $2 \times 10^6$  and  $3.6 \times 10^6$ , based on the free stream velocity and cylinder diameter) covering the supercritical to upper-transition flow regimes around a two dimensional (2D) elliptical cylinder, have been investigated numerically using 2D Unsteady Reynolds-Averaged Navier–Stokes (URANS) equations with a standard high Reynolds number  $k-\epsilon$  turbulence model. The objective of the present study is to evaluate the coefficient of drag along the outer surface of elliptical cylinder with minor-to-major axis ratios of 0.4, 0.6, and 0.8 for different types of velocity input e.g. uniform, parabolic, triangular and plain shear velocity profiles.

The results are compared with published data for circular cylinder in cross flow having uniform velocity. Drag of the elliptical cylinders is lower than a circular cylinder. Reductions in drag may be increased by making the streamlined cylinders more slender. Over the range of Reynolds number considered, an elliptical cylinder with an axis ratio equal to 0.6 reduces drag coefficient by 40 to 45 percent compared to that of a circular cylinder. Although the  $k-\epsilon$  model is known to yield less accurate predictions of flows with strong anisotropic turbulence, satisfactory results for engineering design purposes are obtained for high Reynolds number flows around an elliptical cylinder in the supercritical and upper-transition flow regimes.

**Keywords:** elliptical cylinder; circular cylinder; cross flow; Unsteady RANS; High Reynolds number flows; Navier–Stokes equations.

## Introduction

The phenomenon of flow separation and bluff body wakes has long been intensely studied because of its fundamental significance in flow physics and its practical importance in aerodynamic and hydrodynamic applications. Flow behind a circular cylinder has become the canonical problem for studying such external separated flows. Engineering applications, on the other hand, often involve flows over complex bodies like wings, submarines, missiles, and rotor blades, which can hardly be modeled as a flow over a circular cylinder. In such flows, parameters such as axis ratio, Reynolds number and initial velocity profile can greatly influence the nature of separation and coefficient of drag. A fundamental study of flow over a complex non-canonical object would therefore significantly augment our current understanding of such flows. Due to the complicated nature of the flow, theoretical and experimental analysis is typically limited to flow at very low Reynolds number. Numerical simulations provide a promising approach to analyzing this problem.

Elliptical cylinders ranging from a circular cylinder to a flat plate with changes in axis ratio and provide a richer flow behavior characteristic. There have been a few numerical simulations of flows over elliptic cylinders. Among the few numerical results reported in the open literature are those of Yoshihiro Mochimaru [4] and Zhihua Li et al. [5]. Yoshihiro Mochimaru [4] investigates the effect of Reynolds number and axis ratio on the coefficient of drag and flow streamline prediction for the flow at higher Reynolds number up to  $10^5$ . Zhihua Li et al. [5] applied  $K\omega$ -SST model to study the effect of axis ratio on drag coefficient at  $Re$  up to  $10^4$ . In the absence of comprehensive experimental data for elliptic cylinders for  $Re \geq 5 \times 10^5$ , the present results are in most cases compared against corresponding experimental and numerical data for circular cylinders. Catalano et al. [3] applied 3D Large Eddy Simulation (LES) with wall modeling as well as URANS using the standard  $k$ - $\epsilon$  model of Launder and Spalding [14] with wall functions, for  $0.5 \times 10^6 < Re < 4 \times 10^6$ . Singh and Mittal [7] performed their studies for  $100 < Re < 1 \times 10^7$  using a 2D LES method. Most of the results appear to yield satisfactory agreements with experimental data.

The main objective of the present study is to evaluate the effect of axis ratio and different types of velocity profiles on coefficient of drag, over an elliptical cylinder, using standard  $k$ - $\epsilon$  turbulence model, in the supercritical and upper-transition flow regimes and these results are compared with available experimental data and the numerical results for circular cylinder reported by Catalano et al. [3].

## Mathematical formulation

### Flow model

The Reynolds-averaged equations for conservation of mass and momentum are given by

$$\frac{\partial u_i}{\partial x_i} = 0$$

$$\frac{\partial u_i}{\partial t} + u_j \frac{\partial u_i}{\partial x_j} = -\frac{1}{\rho} \left( \frac{\partial p}{\partial x_i} \right) + \nu \frac{\partial^2 u_i}{\partial x_j^2} - \frac{\partial \overline{u_i u_j}}{\partial x_j}$$

Where  $i, j = 1, 2$ . Here  $x_1$  and  $x_2$  denote the horizontal and vertical directions,

respectively;  $u_1$  and  $u_2$  are the corresponding mean velocity components;  $P$  is the dynamic pressure; and  $\rho$  is the density of the fluid.

The Reynolds stress component,  $\overline{u_1 u_1}$ , is expressed in terms of a turbulent viscosity  $\nu_T$  and the mean flow gradients using the Boussinesq approximation,

$$-\overline{u_1 u_1} = \nu_T \left( \frac{\partial u_i}{\partial x_j} + \frac{\partial u_j}{\partial x_i} \right) - \frac{2}{3} k \delta_{ij}$$

Where  $k$  is the turbulent kinetic energy and  $\delta_{ij}$  is the Kronecker delta function.

A standard high Reynolds number  $k$ - $\epsilon$  turbulence model (see e.g. Launder and Spalding, 1972; Rodi, 1993) is used in the present study; the model has been applied previously on vortex shedding flow by Majumdar and Rodi (1985). The  $k$  and  $\epsilon$  equations are given by:

$$\begin{aligned} \frac{\partial k}{\partial t} + u_j \frac{\partial k}{\partial x_j} &= \frac{\partial}{\partial x_j} \left( \frac{\nu_T}{\sigma_k} \frac{\partial k}{\partial x_j} \right) + \nu_T \left( \frac{\partial u_i}{\partial x_j} + \frac{\partial u_j}{\partial x_i} \right) \frac{\partial u_i}{\partial x_j} - \epsilon \\ \frac{\partial \epsilon}{\partial t} + u_j \frac{\partial \epsilon}{\partial x_j} &= \frac{\partial}{\partial x_j} \left( \frac{\nu_T}{\sigma_\epsilon} \frac{\partial \epsilon}{\partial x_j} \right) + C_1 \frac{\epsilon}{k} \nu_T \left( \frac{\partial u_i}{\partial x_j} + \frac{\partial u_j}{\partial x_i} \right) \frac{\partial u_i}{\partial x_j} - C_2 \frac{\epsilon^2}{k} \end{aligned}$$

Where  $\nu_T = C_\mu (k^2/\epsilon)$ .

The following standard model coefficients have been adopted: ( $C_1 = 1.44$ ,  $C_2 = 1.92$ ,  $C_\mu = 0.09$ ,  $\sigma_k = 1.0$ ,  $\sigma_\epsilon = 1.3$ ).

### Numerical solution procedure, computational domain and boundary conditions

The Reynolds-averaged equations for conservation of mass and momentum, in conjunction with a standard high Reynolds number  $k$  - $\epsilon$  model. A pressures based solver with 1st order discretization in time and 2nd order in spatial is used in this numerical simulation.

The geometric size of the rectangular computational domain and the boundary conditions imposed for all simulations are shown in Fig. 1. The size of the whole computational domain is  $27D \times 14D$ , where  $D$  is the diameter of base circular cylinder. The upper and lower boundaries are located at a distance  $7D$  from the centre of the cylinder; this ensures that these boundaries have no effect on the flow around the cylinder. The flow inlet is located  $7D$  upstream from the centre of the cylinder, and the flow outlet is located  $20D$  downstream from the centre of the cylinder. These distances are sufficient to eliminate the far field effects on the flow upstream and downstream of the cylinder.

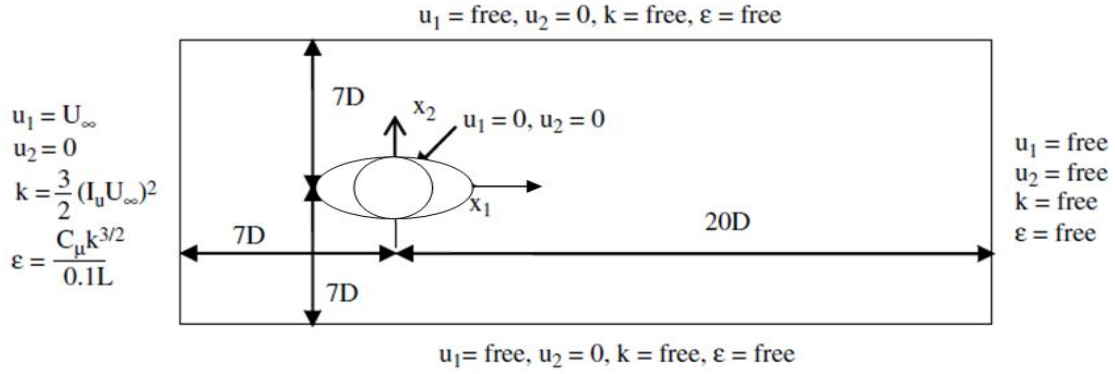


Fig. 1. Computational domain and the imposed boundary conditions

The boundary conditions used for the numerical simulations are as follows:

- (i) Uniform flow is specified at the inlet with  $u_1 = U_\infty$ ,  $u_2 = 0$ . The free stream inlet turbulence values for kinetic energy ( $k = (3/2)(I_u U_\infty)^2$ ) and turbulent dissipation ( $\varepsilon = (C_\mu k^{3/2}) / (0.1L)$ ), proposed by Tutar and Holdø [8], have been imposed.
- (ii) Along the outflow boundary,  $u_1$ ,  $u_2$ ,  $k$  and  $\varepsilon$  are specified as free boundary conditions in a finite element context. This means that a traction-free velocity–pressure boundary condition is applied for  $u_1$ ,  $u_2$  and  $P$ , while the flux is set equal to zero for  $k$  and  $\varepsilon$ .
- (iii) Along the upper and lower boundaries,  $u_1$ ,  $k$  and  $\varepsilon$  are free, while  $u_2$  is set equal to zero.
- (iv) No-slip condition is applied on the cylinder surface with  $u_1 = u_2 = 0$  and standard near-wall conditions are applied for  $k$  and  $\varepsilon$  near the cylinder wall (see e.g. Rodi, 1993) as

$$k = \frac{u_*^2}{\sqrt{C_\mu}}, \quad \varepsilon = C_\mu^{3/4} \frac{k^{3/2}}{kh_p}$$

where  $h_p$  is the radial distance between the first node and the wall,  $k = 0.41$  is the von Karman constant, and  $u_*$  is the wall friction velocity obtained from the logarithmic (log) law.

$$\frac{u_{\tan}}{u_*} = \frac{1}{k} \ln \left( \frac{9h_p u_*}{\nu} \right)$$

is applicable for  $\frac{h_p u_*}{\nu} \geq 30$

Where  $u_{\tan}$  = tangential velocity to the wall.

## Results and Discussion

The computations have been performed at  $Re = 0.5 \times 10^6$ ,  $1 \times 10^6$ ,  $2 \times 10^6$  and  $3.6 \times 10^6$ , covering the supercritical to upper-transition flow regimes. The objective is to evaluate the coefficient of drag variations with minor to major axis ratio for different type of velocity input by using a standard high Reynolds number  $k-\epsilon$  model around an elliptical cylinder and compared with published experimental data and numerical results of circular cylinder (minor to major axis ratio equal to 1).

The presentation which follows is structured to first validate the numerical approach and then to highlight the effect of axis ratio,  $\lambda_0$ , and various velocity profiles on drag coefficient.

### Validation of Numerical Approach

The numerical approach is validated by comparing average values of drag coefficient to prior data for a circular cylinder with  $\lambda_0 = 1$ . The overall drag coefficient is plotted as a function of  $Re$  in Fig. 2.

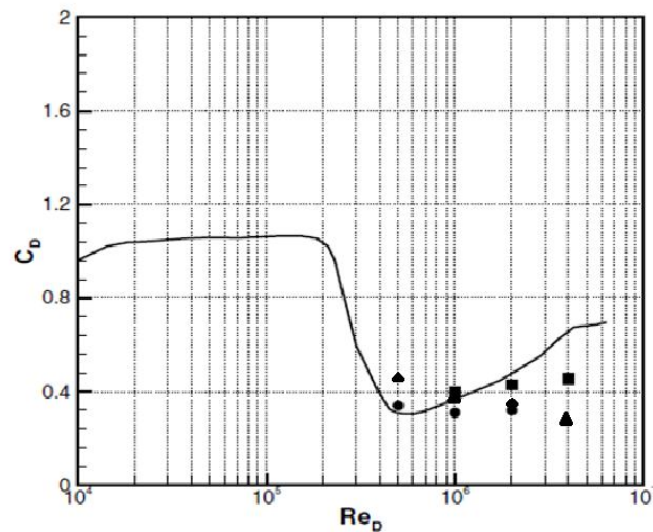


**Fig. 2.** Drag coefficient as a function of the Reynolds number.  
 (—) Achenbach (1968); (●) LES; (■) URANS (▲) present simulation.

The measured data were obtained for a free stream turbulence intensity of 0.8% and turbulent length scale of 0.0045 per unit diameter. The predicted drag coefficient for  $0.5 \times 10^6 \leq Re \leq 2 \times 10^6$  agrees with the experimental and other numerical result but small discrepancies between the present results and the results reported by Catalano et al.[3] are seen at  $3.6 \times 10^6$ . The present computed  $C_D$  decreases slightly as the Reynolds number increases, whereas the URANS and LES results reported by Catalano et al. exhibit a slight increase of  $C_D$ . This might be caused by different implementations of the wall function. The comparisons are shown in Table 1 for  $Re = 1 \times 10^6$ .

Table 1 comparison of numerical and experimental results.

Re = $1 \times 10^6$ (supercritical regime)	CD
Present simulation	0.39
Muk Chen Ong et al. k-epsilon	0.5174
Catalano et al. [3] 3D LES	0.31–0.35
Catalano et al. [3] URANS	0.41
Singh and Mittal [21] 2D LES	0.591
Published experimental data	0.21–0.63

### Parametric Study

Attention is first turned to the effect of streamlined cylinder shape (axis ratio,  $\lambda_0$ ) and different types of velocity profiles on coefficient of drag. Numerical results for elliptical cylinders with  $\lambda_0 = 0.4, 0.6$  and  $0.8$  at  $0.5 \times 10^6 \leq \text{Re} \leq 3.6 \times 10^6$  are compared with the circular cylinders ( $\lambda_0 = 1$ ).

The results are interpreted to determine the conditions under which the shaped cylinder is feasible from the perspective of reducing drag in turbulent cross flow. The impact of Re within the range considered is significant for elliptical cylinders. For streamlined shapes,  $C_D$  decreases as the cylinders are slenderized, i.e.  $\lambda_0$  is decreased. For example, for an elliptical cylinder,  $C_D$  at  $\lambda_0 = 0.4$  is 25% lower than that at  $\lambda_0 = 0.6$  and 60% lower than the circular cylinder. Significant reductions in drag compared to that of the circular cylinder are possible for  $\lambda_0 \leq 0.6$ . To illustrate this point, consider elliptical cylinders with  $\lambda_0 = 0.6$  at  $\text{Re} = 1 \times 10^6$  as shown in fig. 3; drag is reduced by 45% compared to the circular cylinder for any type of input velocity profile.

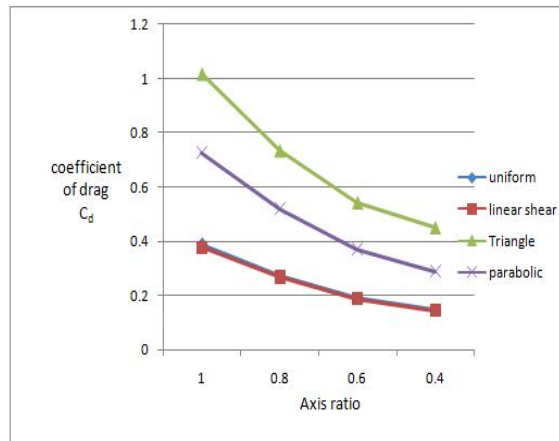


Fig. 3. Coefficient of drag variation with axis ratio at  $\text{Re} = 10^6$ .

For any streamlined cylinder, coefficient of drag for triangular and parabolic velocity input is greater than the uniform and shear velocity input as shown in fig. 3.  $C_D$  curve

for uniform and shear velocity overlaps each other. Coefficient of drag for shear velocity has slightly smaller value than uniform velocity.  $C_D$  for triangular velocity profile is 3 times and for parabolic profile is 1.75 times approximately as compared to uniform velocity.

The variations of coefficient of drag at various axis ratios with Reynolds number for different types of velocity profile are shown in fig. 4. This shows that  $C_D$  decreases as the Reynolds number increases at all axis ratio for any type of initial velocity profiles. These results show better agreement with experimental and numerical results.

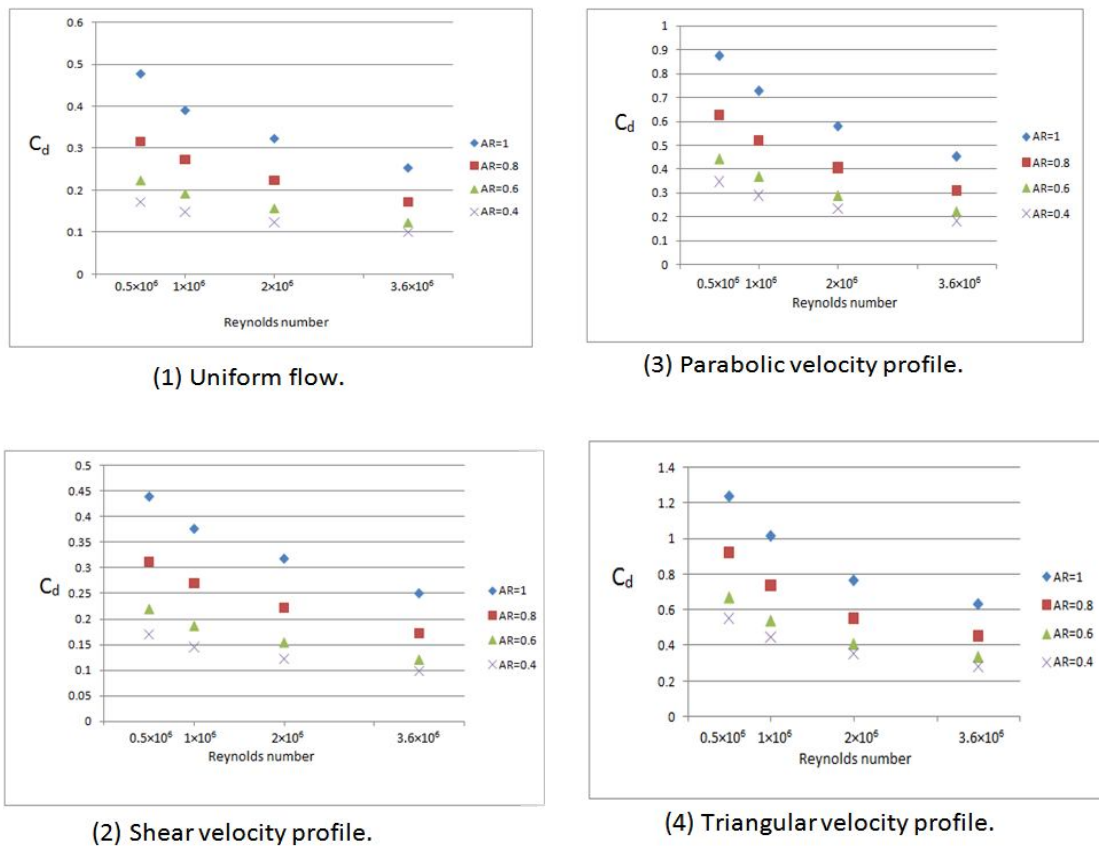


Fig. 4. Coefficient of drag variation with Reynolds number.

Overall, the standard high Reynolds number  $k-\epsilon$  model gives satisfactory predictions of the drag coefficient around a 2D circular and elliptical cylinder in the range  $Re = 0.5 \times 10^6$  to  $3.6 \times 10^6$ . This is based on comparing the results with the published experimental data and numerical results. The results of the present study are encouraging for CFD-based engineering applications, e.g. submarine and wings because the URANS with the standard high Reynolds number  $k-\epsilon$  model requires less computational effort compared with LES and DNS.

## Conclusion

The numerical study of the drag around elliptical cylinders in cross flow with various input velocity profiles for  $0.5 \times 10^6 \leq Re \leq 3.6 \times 10^6$  demonstrate the effects of using streamlined cylinders rather than circular cylinders in different engineering applications. Minor-to-major axis ratios ( $\lambda_o$ ) equal to 0.4, 0.6 and 0.8, are considered for elliptical cylinder. Drag coefficient decreases, as the cylinders are made more slender, i.e.  $\lambda_o$  is decreased. Compared with a circular tube, the drag coefficient is reduced by 40 to 45% by the use of an elliptical cylinder with  $\lambda_o = 0.6$  for any type of velocity profile.

## References

- [1] Achenbach E. Distribution of local pressure and skin friction around a circular cylinder in cross-flow up to  $Re = 5 \times 10^6$ . *J Fluid Mech* 1968; 34(4):625–39.
- [2] Muk Chen Ong, Torbjørn Utnes, Lars Erik Holmedal, Dag Myrhaug, Bjørnar Pettersen, 2008. Numerical simulation of flow around a smooth circular cylinder at very high Reynolds numbers. *Marine Structures* 22 (2009) 142–153.
- [3] Pietro Catalano, Meng Wang, Gianluca Iaccarino, Parviz Moin, 2003. Numerical simulation of the flow around a circular cylinder at high Reynolds numbers. *International Journal of Heat and Fluid Flow* 24 (2003) 463–469.
- [4] Yoshihiro Mochimaru, 1992. numerical simulation of flow past an elliptical cylinder at moderate and high Reynolds numbers, using a spectral method. 11<sup>th</sup> Australasian fluid mechanics conference, Dec 1992.
- [5] Zhihua Li, Jane Davidson and Susan Mantell, Numerical simulation of flow field and heat transfer of Streamlined cylinders in crossflow. *ASME Summer Heat Transfer Conference*, 2005
- [6] R. Mittal and S. Balachandar, Direct Numerical Simulation of Flow Past Elliptic Cylinders. *Journal of computational physics* 124, 351–367 (1996)
- [7] Singh SP, Mittal S. Flow past a cylinder: shear layer instability and drag crisis. *Int J Numer Meth Fluids* 2005;47:75–98.
- [8] Tutar M, Holdø AE. Computational modeling of flow around a circular cylinder in sub-critical flow regime with various turbulence models. *Int J Numer Meth Fluids* 2001;35:763–84.
- [9] Utnes T. Two-equation (k,  $\epsilon$ ) turbulence computations by the use of a finite element model. *Int J Numer Meth Fluids* 1988;8:965–75.
- [10] Utnes T. A segregated implicit pressure projection method for incompressible flows. *J Comp Physics* 2008;227:2198–211.
- [11] Roshko A. Experiments of the flow past a circular cylinder at very high Reynolds number. *J Fluid Mech* 1961;10:345–56.
- [12] Rodi W. Turbulence models and their application in hydraulics. A state-of-the-art review. *IAHR Monograph Series*. 3rd ed. Rotterdam, Netherlands: A.A. Balkema; 1993.
- [13] Majumdar S, Rodi W. Numerical calculation of turbulent flow past circular

- cylinder. In: Proceedings of the 7th turbulent shear flow symposium; 1985. p. 3.13–25. Stanford, USA.
- [14] Launder BE, Spalding DB. Mathematical models of turbulence. London: Academic Press; 1972.
- [15] Shuyang Cao, Yukio Tamura, Flow around a circular cylinder in linear shear flows at subcritical Reynolds number. *Journal of Wind Engineering and Industrial Aerodynamics* 96 (2008) 1961–1973